Julio A. Deiber[1]
Maria V. Piaggio[2]
Marta B. Peirotti[1]

[1]Instituto de Desarrollo Tecnológico para la Industria Química (INTEC), Universidad Nacional del Litoral (UNL), Consejo Nacional de Investigaciones Científicas y Técnicas (CONICET), Santa Fe, Argentina
[2]Cátedra de Bioquímica Básica de Macromoléculas, Facultad de Bioquímica y Ciencias Biológicas, UNL, Santa Fe, Argentina

Received July 26, 2012
Revised October 2, 2012
Accepted October 17, 2012

Research Article

Determination of electrokinetic and hydrodynamic parameters of proteins by modeling their electrophoretic mobilities through the electrically charged spherical porous particle

This work explores the possibility of using the electrically charged "spherical porous particle" (SPP) to model the electrophoretic mobility of proteins in the low charge regime. In this regard, the electrophoretic mobility expression of the charged SPP (Hermans–Fujita model) is used and applied here to BSA and staphylococcal nuclease for different protocol pH values. The SPP is presented within the general framework of the "spherical soft particle" as described in the literature. The physicochemical conditions required to model proteins as SPP from their experimentally determined electrophoretic mobilities are established. It is shown that particle permeability and porosity and chain packing and friction fractal dimensions are relevant structural properties of proteins when hydrodynamic interaction between amino acid residues is present. The charge regulation phenomenon of BSA and staphylococcal nuclease with p*I*s $\approx$ 5.71 and 9.63, respectively, is described through the SPP within a wide range of bulk pH values. These case studies illustrate when the average regulating $\langle pH \rangle$ of the protein domain is lower and higher than the protocol pH. Further research for using the general spherical soft particle is also proposed on the basis of results and main conclusions.

Keywords:
Polyampholyte spherical porous particle / Polyampholyte spherical soft particle / Polypeptide permeability / Protein electrical charge regulation / Protein electrophoretic mobility
DOI 10.1002/elps.201200405

Additional supporting information may be found in the online version of this article at the publisher's web-site

1 Introduction

At present, many data of polyampholyte-polypeptide electrophoretic mobility μ_p obtained from CZE in different BGEs are available in the literature (see, for instance, [1–5] and citations therein). A number of them were achieved in BGEs having values of pH and ionic strength I involving the low charge regime, where a linear relationship between electrophoretic mobility and surface potential may be approximately established. Thus, in this regime ion polarization-relaxation due to the flowing BGE around the electrically driven particle may be neglected [6, 7]. For a discussion on this aspect see, for instance, Refs. [8–10]. From the theoretical point of view, the electrophoretic mobility model involving the charged spherical hard particle in the low charge regime can be used to interpret experimental μ_p values (designated μ_p^{exp} here). Thus, Henry electrophoretic mobility μ_p^H is expressed as follows [11]:

$$\mu_p^H = \frac{2}{3}\frac{\varepsilon\zeta}{\eta_s} f_H(\kappa\, a_H) \tag{1}$$

Equation (1) involves electrical permittivity ε, viscosity η_s, and temperature T of BGE, Debye–Hückel parameter $\kappa = \sqrt{2e^2 I N_A 10^3/(\varepsilon k_B T)}$, Stokes hydrodynamic radius a_H, and Henry function $f_H(\kappa a_H)$. The zeta potential $\zeta = eZ/(4\pi\varepsilon a_H(1+\kappa a_H))$ is obtained from the solution of the linearized Poisson–Boltzmann equations. Here, e is the

Correspondence: Dr. Julio A. Deiber, INTEC, Güemes 3450, S3000GLN, Santa Fe, Argentina
E-mail: treoflu@santafe-conicet.gov.ar
Fax: +54-342-4550944

Abbreviations: AAS, amino acid sequence; **AHP**, aspherical hard particle; **PLLCEM**, perturbed Linderstrøm-Lang capillary electrophoresis model; **SPP**, spherical porous particle; **SSP**, spherical soft particle; **STN**, staphylococcal nuclease

© 2013 WILEY-VCH Verlag GmbH & Co. KGaA, Weinheim

elementary charge, N_A is Avogadro constant, and k_B is Boltzmann constant. Thus, one requirement for this approximation is that the polypeptide effective charge number $Z = \sum_i Z_i n_i$ must be relatively small, where Z_i and n_i are the charge number and the number of each i-ionizing group of amino acid residues in the polypeptide chain, respectively, including $-NH_2$ and –COOH terminal groups. To improve the prediction of Eq. (1) when polypeptides are considered, the perturbed Linderstrøm-Lang capillary electrophoresis model (PLLCEM) was proposed [6, 7, 12–16], where electrophoretic mobilities of aspherical hard particles (AHPs) were studied in the low charge regime, by defining the shape orientation factor $\Omega = \mu_p/\mu_p^H \approx 6\pi\eta_s a_H/f$. Here, the friction coefficient is evaluated either from AHP, such as spheroidal particles, or from hydrated chain fractals by defining the chain friction $f = 6\pi\eta_s a_o N^{g_f}$, where g_f is the friction fractal dimension and a_o is the average radius of *N* amino acid residues in the amino acid sequence (AAS) evaluated from their van der Waals radii. Also in this framework the packing fractal dimension is $g_p = \log N/\log(a_H/a_o)$ as defined in [6, 15, 16]. This simple CZE model yields approximate numerical values of useful polypeptide properties, apart from a_H, Ω, f, and Z, when chain AAS and molar mass M are known. In fact, it is also possible to estimate average values of hydration δ and specific volume v_p of polypeptides. For these purposes, polypeptides are modeled as a chain of *N* beads, where each amino acid residue size is associated with the radius a_o (important details are provided in [17–19]). From previous works, one concludes that AHP and hydrated chain fractals can model proteins by describing phenomena associated with their size, shape, average orientation during particle migration, electrical charge of weak ionizing groups confined at the particle surface [12, 14, 15], and particle hydration related to the degree of protein denaturation and the presence of ionizing polar and nonpolar amino acid residues. These characteristics were also shown to be relevant for the estimation of polypeptide diffusion coefficient and intrinsic viscosity [7, 15].

By considering the above analysis, this work explores the possibility of using an electrically charged spherical porous particle (SPP) to model the electrophoretic mobility of polypeptides in the low charge regime. In this regard, the Hermans–Fujita analytic expression of μ_p provided and widely analyzed by Ohshima [20–25] is used and applied here specifically to proteins, in conjunction with theoretical aspects concerning the charge regulation phenomenon already described in the PLLCEM [6, 7, 12, 13, 15]. Thus, in this first study on polyampholyte-polypeptide SPP, particular numerical codes, where model parameters may also vary within the particle, are not considered [26, 27]. It is relevant to point out that the "spherical soft particle" (SSP) behaves asymptotically as two extreme particle types: spherical hard particle and SPP, which correspond to Henry and Hermans–Fujita electrophoretic mobility models in the low charge regime, respectively. Since we keep working in this regime, once more ion polarization-relaxation of the BGE is neglected in the present framework. In particular, this complex phenomenon has been already studied in the electrophoresis of charged SSP through numerical models including applications to colloidal particles and biological cells [28–30]. Further relevant asymptotic responses for highly charged SSP were provided in [31].

From the general SSP and by following closer the developments and nomenclature in [20–23], it is clear that this particle type is composed of an uncharged core of radius a covered by a polymeric layer of thickness $d = b - a$ (designated polyampholyte layer throughout this work), where b is the radius of the whole particle. Therefore, the characteristic magnitudes considered in the modeling of the electrophoretic mobility of SSP are the friction density γ evaluating the resistance offered to the flow of BGE solution by chain segments distributed in the layer of thickness d. In this regard, it is convenient to define parameter $\lambda = (\gamma/\eta_s)^{1/2}$, providing the particle softness λ^{-1} [20, 21], and the constant fixed charge density $\rho_{fix} = 3eZ/[4\pi(b^3 - a^3)]$ uniformly distributed throughout the polymeric layer as simpler case (see also [26, 27, 32] for more general considerations). Here, we add that the polypeptide mass must be distributed between the particle core and polyampholyte layer requiring $a < a_c$, where $a_c = \{3Mv_p/(4\pi N_A)\}^{1/3}$ is the protein compact radius defined in [15]. These expressions also imply that the chain molar mass $M_d = 4\pi(a_c^3 - a^3)N_A/(3v_p)$ located in the polyampholyte layer is a fraction of the total polypeptide molar mass M. The constraint $a < a_c$ is also useful to analyze protein hydration $\delta = ((b/a_c)^3 - 1)v_p/v_w$ (mass of water per mass of protein) and physical aspects associated with the existence of a particle core in the SSP composed mainly of hydrophobic amino acid residues, although they may still have associated some hydration on physical grounds as discussed in [15, 33–36]. In the present work, we study in particular the SPP that implies that $a = 0$. Thus, the use of SPP is an appropriate starting point to model a protein electrophoretic mobility within the wider framework of the SSP, allowing, in principle, to assign a polypeptide hydration uniformly distributed in the whole particle. We present the application of the SSP to the modeling of electrophoretic mobility of polypeptides in [37].

From the above framework, one expects to find a clear interplay among polypeptide AAS, parameters of the charged SPP and SSP, polypeptide permeability, and physicochemical properties of BGEs. Furthermore, similar values of proteins physicochemical properties obtained through classical experimental techniques shall be calculated with these models to get physical consistency. In addition, when the electrophoretic mobility of other particles different from proteins is considered (for instance, synthetic colloids) one has available as input data less-defined properties. In this regard, a typical fitting parameter is the effective particle charge number *Z* or the charge density ρ_{fix}, which need to be estimated because, in principle, the number of charged groups in the particle is unknown. In contraposition to this situation, the knowledge of the polypeptide AAS provides a good estimation of *Z* value once the protocol pH and I of the BGE have been fixed and the protein charge regulation phenomenon has been included (see [6] and citations therein).

This work is organized as follows. In Section 2, some theoretical aspects involving the electrophoretic mobility

© 2013 WILEY-VCH Verlag GmbH & Co. KGaA, Weinheim

Table 1. Numerical estimations of electrokinetic and hydrodynamic properties of BSA through the Hermans–Fujita model as a function of bulk pH at 25°C

pH	3	4	7	8	9	10	11
$\mu_p \times 10^8 (\frac{m^2}{Vs})$	2.77	1.50	− 1.73	− 2.25	− 2.68	− 3.03	− 3.18
b(Å)	70.38	70.33	34.11	37.64	37.59	41.41	55.87
δ	12.54	12.51	0.80	1.32	1.31	1.99	5.92
H_d	44890	44660	1325	3240	3219	5743	20280
H	46242	46138	2949	4860	4834	7340	21825
$\langle pH \rangle$	3.81	4.44	6.52	7.36	8.23	9.11	10.04
$\langle \psi \rangle$(mV)	48.00	26.02	− 28.38	− 38.02	− 45.36	− 52.43	− 56.78
Z	71.60	38.75	− 10.18	− 16.23	− 19.32	− 26.66	− 51.82
Z_w	93.96	62.50	− 14.35	− 18.47	− 25.06	− 50.31	− 87.48
$\rho_{fix} \times 10^{-7}$ (C/m^3)	0.79	0.43	− 0.98	− 1.16	− 1.39	− 1.44	− 1.14
τ	0.96	0.96	0.63	0.73	0.73	0.80	0.92
$K \times 10^{19}$ (m^2)	8.37	8.36	3.90	4.06	4.06	4.30	5.79
g_p	2.00	2.00	2.59	2.49	2.49	2.40	2.16
g_f	0.90	0.90	0.68	0.72	0.72	0.76	0.85
$\lambda \times 10^{-9}$(m^{-1})	1.09	1.09	1.60	1.57	1.57	1.52	1.31

For the meaning of all symbols presented, please see the text, where they are first defined, or the total list of symbols in the Supporting Information.
The following constants are used: $N = 583$, $v_p = 0.708$ cm^3/g, M = 66387 g/mol, $a_o = 2.92$ Å, $a_c = 26.51$ Å, p$I = 5.71$, and I $\approx$ 10 mM. The protein permeability is calculated through Eq. (10).

Table 2. Numerical estimations of electrokinetic and hydrodynamic properties of STN through the Hermans–Fujita model as a function of bulk pH at 25°C

pH	2.8	4.1	5.7	6.8	8.9
I (mM)	5.5	55	36	26	14
$\mu_p \times 10^8 (\frac{m^2}{Vs})$	2.45	2.04	1.85	1.81	1.31
b(Å)	64.11	35.69	29.71	27.41	23.59
δ	38.87	6.12	3.23	2.38	1.26
H_d	35900	5300	2577	1790	753
H	36266	5706	3012	2223	1177
$\langle pH \rangle$	3.37	4.46	6.07	7.18	9.19
$\langle \psi \rangle$(mV)	33.83	21.06	22.03	22.77	17.19
Z	30.17	19.81	10.79	8.12	3.72
Z_w	32.14	23.84	11.92	8.84	5.17
$\rho_{fix} \times 10^{-7}$ (C/m^3)	0.44	1.67	1.57	1.51	1.08
τ	0.99	0.92	0.86	0.82	0.72
$K \times 10^{19}$ (m^2)	18.28	5.84	4.73	4.42	4.02
g_p	1.62	2.00	2.15	2.23	2.39
g_f	0.94	0.82	0.75	0.71	0.64
$\lambda \times 10^{-9}$(m^{-1})	0.74	1.31	1.45	1.50	1.58

For the meaning of all symbols presented, please see the text, where they are first defined, or the total list of symbols in the Supporting Information.
The following constants are used: $N = 149$, $v_p = 0.712$ cm^3/g, M = 16792 g/mol, $a_o = 2.91$ Å, $a_c = 16.79$ Å, p$I = 9.63$. The protein permeability is calculated through Eq. (10).

modeling of the general electrically charged SSP [20–25] are described for the purposes of visualizing those corresponding to the SPP as a particular case of the SSP and for a clear presentation of the general framework in [37]. Thus, the simple case of a SPP may be useful at this stage to establish the interplay between the physicochemical properties of proteins and particle characteristic parameters when $a = 0$. Also, additional physical considerations are provided to make feasible the comparison between predictions of SPP at different pH values. In Section 3, the discussion of results is presented indicating the conditions under which a polyampholyte-polypeptide electrophoretic mobility may be modeled through a charged SPP. Here, the globular proteins used as case studies are BSA [38] and staphylococcal nuclease (STN) [39] at 25°C. The experimental electrophoretic mobility data of these proteins are reported in the literature cited for different protocol pH values (see also Tables 1 and 2). Although the temperature value was not explicitly reported in [38], calculations of thermophysical properties indicated a temperature closed to 25°C. Also a critical analysis of

© 2013 WILEY-VCH Verlag GmbH & Co. KGaA, Weinheim

numerical results is carried out and subjects for future research are proposed. Concluding remarks are provided in Section 4 to highlight the importance of modeling electrophoretic mobility of polypeptides to understand better physicochemical mechanisms associated with transport properties of this type of chain, mainly in biological systems.

Before ending this section, we point out that the motivation of the present work is based on the fact that previous theoretical studies modeling polypeptide electrophoretic mobility considered particle types being able to describe different phenomena associated with electrokinetic and hydrodynamic responses of polyampholyte chains migrating in an applied electrical field. In this framework, the estimation of polypeptide properties through particles models is relevant once the AAS is known. Therefore, in this work and following one [37], we have the target of analyzing different particles (SPP and SSP) to obtain as main result the particle–solvent friction for different chain conformations. Then this parameter may be interpreted through the "hydrated chain fractal" model (as it was done for the AHP in [6, 15, 16]) to evaluate the packing and friction fractal dimensions of polypeptide chains, which in turns are crucial to examine polypeptide global conformations and scaling laws at different pH values. These scaling laws relate chain electrophoretic mobility to intrinsic viscosity, diffusion and sedimentation coefficients, and particle permeability in different polypeptide conformational states [6, 7, 37]. In fact, the values of friction fractal dimension are shown below to be sensitive to the type of particle used to cover the collapsed to free draining chain states.

2 Modeling

The theoretical framework providing asymptotic and analytic electrophoretic mobility expressions associated with the general charged SSP in the low charge regime involves several hypotheses stated in [20–23]. Additional considerations are also introduced here to allow, in principle, the application of this particle model to polyampholyte-polypeptide chains [6, 7]. In general, the required hypotheses are as following: (i) The BGE is considered an incompressible fluid and the creeping flow approximation to Navier–Stokes equation is valid outside and inside the polyampholyte layer. In this layer, the Darcian term is incorporated, while both domains include the electrostatic force on free ions suspended in the solvent. (ii) The low charge regime is considered, where a linear relation between electrophoretic velocity and applied electrical field is approximately valid. (iii) The shear plane with nonslip fluid velocity is located on the particle core surface. Thus, the so-called "Brickman term" is included in the layer zone. (iv) Electrolyte-free ions cannot penetrate the particle core (in principle, the particle core is assumed anhydrous). (v) The polymeric layer is permeable to BGE ions. We also add here the fact that this layer may be composed mainly by polyampholyte strands with positive and negative weak ionizing groups as long as polypeptide particles are concerned. (vi) The electrical permittivity is approximately the same inside the polyampholyte layer and outside in the BGE solution. This consideration simplifies the estimation of the charge regulation phenomenon of weak ionizing groups by neglecting approximate perturbations terms associated with electrical permittivity changes (see, for instance, details in [6] and citations therein). (vii) Weak i-ionizing groups in the polyampholyte layer are partially dissociated and their charge numbers Z_i are quantified from reference pK_i^r and average regulating $\langle pH\rangle$ giving ΔpK shift values [12]. As a consequence of hypothesis (vi), the charge regulation phenomenon around protein ionizing groups allows one the estimation of $\langle pH\rangle$ as follows [12]:

$$\langle pH\rangle = pH + \frac{e\langle\psi\rangle}{\ln(10)\, k_B T} \tag{2}$$

where $\langle\psi\rangle$ is the average value of the equilibrium particle electrical potential evaluated in the polyampholyte layer through:

$$\langle\psi\rangle = \frac{3}{(b^3 - a^3)} \int_a^b \psi^{(o)}(r)\, r^2 dr \tag{3}$$

Here, the equilibrium electrical potential $\psi^{(o)}(r)$ for $a < r < b$ is used as reported in [20, 23]:

$$\psi^{(o)}(r) = \frac{\rho_{fix}}{\varepsilon\kappa^2}\left\{1 - \left(\frac{1+\kappa b}{1+\kappa a}\right)\exp[-\kappa(b-a)] \times\left(\frac{\sinh[\kappa(r-a)]}{\kappa r} + \frac{a\cosh[\kappa(r-a)]}{r}\right)\right\} \tag{4}$$

(viii) BGE polarization-relaxation effects are negligible because the electrostatic fields inside and outside the particle are rather low. (ix) The Darcian friction density γ in the polyampholyte layer is constant. In this framework, two general analytic expressions for the electrophoretic mobility of a charged SSP were provided by Ohshima [20, 23]. They may be briefly represented through the following function:

$$\mu_p = \prod_{r=a}^{\infty}(a, b, \lambda, G(r, \psi_o)) \tag{5}$$

where $G(r, \psi_o) = -(\varepsilon\kappa^2/\eta_s)\{1 + a^3/(2r^3)\}\, d\psi^{(o)}/dr$, as deduced in [20–23]. Also:

$$\psi_o = \frac{\rho_{fix}}{2\varepsilon\kappa^2} \times\left\{1 - \frac{1}{\kappa b} + \frac{(1-\kappa a)(1+\kappa b)}{(1+\kappa a)\kappa b}\exp[-2\kappa(b-a)]\right\} \tag{6}$$

is the surface electrical potential at $r = b$. In one of the general analytic expressions, the electrical force on the BGE due to the applied external electrical field and the solvent force on the polyampholyte layer balanced each other [20]. In the other expression, the BGE pressures evaluated at $r = b$ from the polyampholyte layer and from the BGE solution sides must be equal [23] (see also additional details in [27]). Interesting is the fact that both models yield the same asymptotic expressions as reported in [20–23], although the later one is preferred [22]. Further, in these citations the use of the asymptotic response of these models for $\lambda \to \infty$ indicates that no flow of the BGE solution through the polyampholyte layer

© 2013 WILEY-VCH Verlag GmbH & Co. KGaA, Weinheim

of thickness d is obtained. Nevertheless, emphasis must be placed on the fact that the diffusion fluxes of BGE-free ions in and out of this layer are still allowed. For this reason, when $\lambda \to \infty$ in these models one refers to the "spherical semisoft particle" [23]. Only in this regard, one finds that this particle of null softness may be related in nature to spherical hard particles, which may be in particular studied through the PLLCEM framework. In this work, we concentrate in the case where the particle core is null ($a = 0$). This asymptotic case yields the SPP electrophoretic mobility expression [21, 23] as follows:

$$\mu_p = \frac{\rho_{fix}}{\eta_s \lambda^2}\left\{1 + \frac{1}{3}\left(\frac{\lambda}{\kappa}\right)^2\left(1 + \exp(-2\kappa b) - \frac{(1-\exp(-2\kappa b))}{\kappa b}\right)\right.$$
$$\left. + \frac{1}{3}\left(\frac{\lambda}{\kappa}\right)^2 \frac{[1+1/(\kappa b)]}{[(\lambda/\kappa)^2 - 1]}\left[\left(\frac{\lambda}{\kappa}\right)\frac{[1+\exp(-2\kappa b) - (1-\exp(-2\kappa b))/(\kappa b)]}{[(1+\exp(-2\lambda b))/(1-\exp(-2\lambda b)) - 1/(\lambda b)]} - (1-\exp(-2\kappa b))\right]\right\} \quad (7)$$

Equation (7) was first derived by Hermans and Fujita [40] for charged porous spheres.

In relation to protein hydration, the total number of water molecules per polypeptide chain $H = \delta M/18$ shall be equal to the water molecules captured by amino acid residues of the polypeptide AAS plus the number of water molecules H_d due to the degree of protein denaturation. These values depend on protocol pH, as it is demonstrated below. Thus, the following expressions and equality may be used as a first approximation to this complex phenomenon [35]:

$$H = h^I_{t\text{-}COOH}|Z_{COOH}| + h^I_{t\text{-}NH_3^+}\left|Z_{NH_3^+}\right| + h^{PI}_{t\text{-}COOH}(1 - |Z_{COOH}|) + h^{PI}_{t\text{-}NH_3^+}(1 - Z_{NH_3^+}) + \sum_i^N \left\{h^I_i|Z_i| + h^{PI}_i(1-|Z_i|) + h^P_i + h^{NP}_i\right\} + H_d$$
$$= M((b/a_c)^3 - 1)v_p/(18v_w) \quad (8)$$

where h^I_i and h^{PI}_i are the number of water molecules of ionizing and polar-ionizing i-amino acid residues, weighed through their charge number $Z_i = \pm 1/(1 + 10^{\mp(pK^r_i - \langle pH\rangle)})$ as a consequence of their twofold electrostatic character, while h^P_i and h^{NP}_i stand for the number of water molecules of polar and nonpolar i-amino acids residues, respectively. In Eq. (8), $h^I_{t\text{-}COOH}$, $h^I_{t\text{-}NH_3^+}$, $h^{PI}_{t\text{-}COOH}$, and $h^{PI}_{t\text{-}NH_3^+}$ are the corresponding values for ionizing and polar-ionizing terminal groups (see [13, 35] for further details on the estimation of reference pK_i designated pK^r_i and the numbers of water molecules). It is also clear that the effective protein charge number is $Z = \sum_i n_i Z_i$, where the summation is carried out for all the ionizing groups in the AAS.

The closure of the SPP electrophoretic mobility model (Eq. 7) requires a value for λ. Therefore, as a first approximation the evaluation of $\lambda \approx 1/K^{1/2}$ is carried out from expressions of the average permeability K available in the literature (see [32] and citations therein). For instance, the so-called dilute model provides:

$$K \approx 2a_o^2 \Big/ (9\tau_p) \quad (9)$$

where $\tau_p \approx N(a_o/b)^3$ is the polypeptide volume fraction in the hydrated SPP domain and $\tau \approx 1 - \tau_p$ is the SPP porosity. When hydrodynamic interaction between pairs of amino acid residues is important, the following permeability expression is used [41–43]:

$$K = \frac{2a_o^2}{9\tau_p}\left(1 + \frac{3}{\sqrt{2}}\tau_p^{1/2} + \frac{135}{64}\tau_p \ln\tau_p + 16.45\tau_p + \cdots\right) \quad (10)$$

where leading terms of the sum are considered [43]. From previous definitions in [6, 15, 16], one also finds that K is related to the packing and friction fractal dimensions through $\tau_p \approx (a_o/b)^{3-g_p}$ and $g_f = \log(2b^3/9a_oK)/\log(N)$, respectively. Thus, asymptotically $g_f = 1$ for the free draining dilute model (Eq. 9).

Equations (2)–(4) and (6)–(10) were used in a simple numerical code to fit experimental data of the electrophoretic mobility of BSA and STN at different pH values. In this regard, the main difficulty in solving these problems was to define the input data associated with specific polypeptide case studies considered here. Therefore, for $a = 0$ and $M_d = M$, trial values of b and H_d are iterated until Eq. (8) is satisfied and the calculated mobility μ_p (Eq. 7) converges to the experimental mobility μ_p^{exp} within an acceptable relative error around 10^{-3}. The Supporting Information presents a brief description of this numerical code. Once the problem has been solved, complementary parameters and properties are evaluated.

3 Results and discussion

Numerical values of $\rho_{fix} = 3eZ/(4\pi b^3)$ may be obtained for BSA and STN as reported in Tables 1 and 2 (see also Supporting Information Tables 1 and 2) by using a numerical code involving Hermans–Fujita model (Eq. 7) where $a = 0$. One thus finds that these proteins at the pH and I of the CZE protocols reported in [38, 39] have absolute values of ρ_{fix} comprised approximately between 0.027 and 0.266 elementary charge per nm^3, which are expected values by taking into account that these particles are in the low charge regime. Table 1 shows numerical predictions of the SPP model for BSA, where Eq. (10) for protein permeability is used. Model parameters and physicochemical properties show a significant dependence on pH as expected. It is interesting to point out that the SPP radius is minimized at around the protein native state at pH 7 by yielding $b \approx 34.11$ Å, which is a typical value for the native BSA. At this pH, in addition, the protein hydration $\delta \approx 0.80$ is also a minimum value consistently with the fact that at higher and lower pH than that of the native

© 2013 WILEY-VCH Verlag GmbH & Co. KGaA, Weinheim

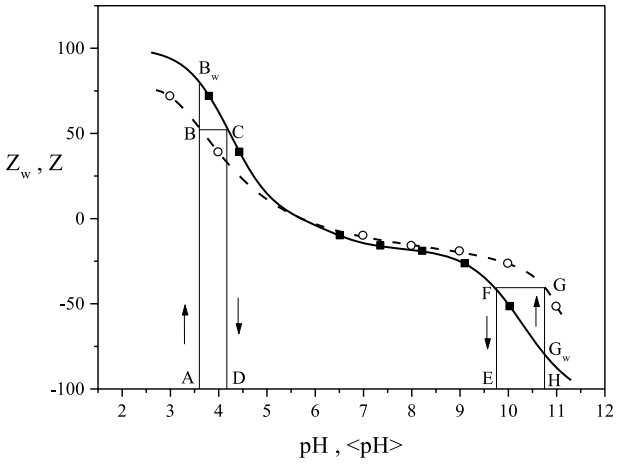

Figure 1. Effective wild charge number Z_w as a function of bulk pH (full line) for BSA. Dashed line indicates the effective regulated charge number Z as a function of bulk pH, obtained by fitting numerical results (symbols (○)) predicted with the SPP model for increasing bulk pH 3, 4, and 7–11, respectively (Table 1). Symbols (■) are also numerical results of effective regulated charge number Z as a function of average particle ⟨pH⟩. Path ABCD provides the effective regulated charge number Z (points B or C) and average particle ⟨pH⟩ (point D) for a given bulk pH (point A) below the p*I*. Path EFGH shows the opposite situation for pH > p*I*. Points B_w and G_w indicate values of wild charge number Z_w for bulk pH values at points A and H, respectively. The numerical p*I* estimated is 5.71. Equation (10) for protein permeability is used (see also Table 1).

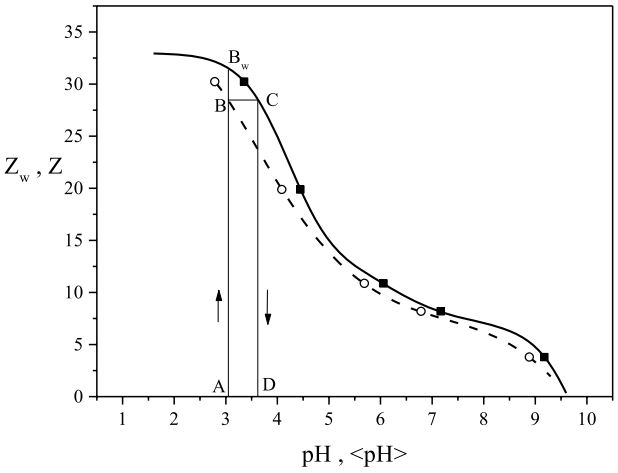

Figure 2. Effective wild charge number Z_w as a function of bulk pH (full line) for STN. Dashed line indicates the effective regulated charge number Z as a function of pH obtained by fitting numerical results (symbols (○)) predicted with the SPP model for increasing bulk pH 2.8, 4.1, 5.7, 6.8 and 8.9, respectively (Table 2). Symbols (■) are also numerical results of effective regulated charge number Z as a function of average particle ⟨pH⟩. Path ABCD provides the effective regulated charge number Z (points B or C) and ⟨pH⟩ (point D) for a given bulk pH (point A). Point B_w indicates the wild charge number Z_w for the bulk pH (point A). The numerical p*I* estimated is 9.63. Equation (10) for protein permeability is used (see also Table 1).

state one expects to find protein denatured states. In these regards, Table 1 shows that δ may be as high as 12.54 and 5.92 for the extreme pH 3 and 11, respectively, where the protein suffers an important denaturation mainly due to repulsing electrostatic forces at high positive and negative effective charge numbers ($Z \approx 71.60$ and -51.82, respectively). Thus, protein destabilization from the collapsed globule regime toward the hybrid and polyelectrolyte regimens are expected as discussed in [6]. These results are consistent with the high numbers of water molecules H and H_d residing in the SPP, the relatively low packing fractal dimensions and the high porosities obtained at these extreme pH values as reported in Table 1. This table also illustrates the effect of protein p*I* value through properties such as ⟨ψ⟩, Z, ρ_{fix}, and Z_w that change sign for pH > 5.71. Here, Z_w is designated "wild charge number" as obtained directly from theoretical titration without accounting for protein charge regulation. Apart from these results demonstrating mainly the physical consistency of numerical predictions associated with the SPP model, it is relevant to observe that the charge regulation phenomenon manifests with a pH change that is quantitatively different below and above the protein p*I*, as depicted in Fig. 1 for BSA. For instance, in this figure the path ABCD indicates the charge regulation phenomenon occurring for pH < p*I*. Consequently, this path provides both the effective regulated charge number Z (points B or C) and the average regulating ⟨pH⟩ (point D) for the given bulk pH (point A) below the p*I*, thus resulting ⟨pH⟩ greater than pH and $Z < Z_w$. In fact, for pH < p*I* the SPP is effectively positive and hence relatively deficient in hydrogen ions when compared with the BGE solution. Point B_w in Fig. 1 indicates the wild charge number Z_w for the bulk pH (point A) in the path ABCD. On the other hand, path EFGH shows the opposite situation for pH above the p*I*, giving ⟨pH⟩ lower than pH and $Z > Z_w$ (for pH > p*I*, the SPP is effectively negative and hence relatively abundant in hydrogen ions when compared with the BGE solution). These results demonstrate that the protein domain has not the same pH as that of the BGE solution and that ⟨pH⟩ approaches the bulk pH near the p*I* only. For STN, Fig. 2 shows that path ABCD is present only because the p*I* 9.63 for this protein is relatively high to be able to take negative effective charge numbers in the experimentation range. These results are compatible with the charge regulation phenomenon already described in [12,15]; for the particular case, one assumes the protein charge is confined at the hard particle surface and the zeta electrical potential ζ is considered. In this regard, the SPP presents the advantage that the electrical charge is distributed throughout the particle volume in a closer approximation to actual protein particles (see discussion in [15]). It is interesting to point out that results reported in Tables 1 and 2 show that BSA and STN behave SPP quite well, with values of particle sizes suitable from the physical point of view and also satisfying $b > a_c$.

The other relevant physical aspects found in Tables 1 and 2 are that the ranges of values taken by parameters λ, K, τ, and g_p provide information concerning the conformational states of proteins according to bulk pH values. For instance, for the BSA, Table 1 shows that the lower protein

© 2013 WILEY-VCH Verlag GmbH & Co. KGaA, Weinheim

permeability (similarly the lower SPP softness) is obtained at pH 7 as expected for the rather native state of this protein with $K \approx 3.90\ 10^{-19}$ m^2. This also implies that at this pH the SPP porosity is a minimum value with $\tau \approx 0.63$. Here, it must be observed that the charge regulation phenomenon shifts the average regulating ⟨pH⟩ toward values closer to the protein p*I* when pH ≈ 7. At the very acid and alkaline limits of the BGE solution the protein porosity takes quite high values, for instance, $\tau \approx 0.96$ and 0.92, respectively, indicating that the polyelectrolyte regime has been reached [6]. These results are well suited with the high hydration values obtained and reported in Table 1 for denatured BSA. Other models providing relatively lower values of permeability were also tested here for the proteins under study, such as the dilute model [32] giving intermediate K values (see Supporting Information Tables 1 and 2 for BSA and STN, respectively), and Happel model [44] for even lower K values. These models, however, did not allow the matching of the experimental electrophoretic mobility at those pH values close to the p*I* when BSA and STN were considered (in particular, BSA has the native state at around one unit of pH above its p*I*). In fact, the use of Eq. (10) indicates that amino acid hydrodynamic interactions seem to be important for these two proteins. Also numerical results show that the protein softness reported in Tables 1 and 2 is rather low approaching the p*I*, implying a polyampholyte domain with a quite low Darcian permeability for the BGE solution flow. Thus, the low permeability values for these proteins in the framework of classical porous medium theories would yield a rather weak flow. The application of the charged SSP electrophoretic mobility model for higher particles such as biological cells, yielded higher softness of order $\lambda^{-1} \approx 10^{-7}$ to 10^{-9} m [45].

The analysis of the power friction coefficient g_f quantified from the average protein permeability values calculated here is important to understand polyampholyte-polypeptide chain conformations. In fact Tables 1 and 2 show that $3/5 < g_f < 1$ for BSA and STN. Thus, the polypeptide SPP gives consistently chain conformations above the Flory theta-point defined at $g_f \approx 1/2$. Previously, we found that when the friction of polypeptide AHP is interpret through a hydrated fractal chain the result was $1/3 < g_f < 3/5$ [6, 7, 16]. In these regards, it is clear that around $g_f \approx 3/5$ amino acid hydrodynamic interaction due to solvent flow through the particle is enhanced. Thus, both particles with different physical natures are explaining in part the wide range of values taken by the polypeptide intrinsic viscosity, scaling according to $[\eta] \propto N^{\nu}$, where $\nu = 3g_f - 1$ is the Mark–Houwink exponent (see also details in [7]). Therefore, these particles would be allowing $0 < \nu < 2$, from the collapsed globule to the free draining chain regimes. In general, the free draining dilute model (Eq. 9) for K having $g_f = 1$ is not appropriate for pH values near the protein p*I* (see Supporting Information Tables 1 and 2).

From a more general point of view, it is clear that BSA and STN near their native states are within the collapsed globule regime [6, 7], and hence they may be also studied through the general SSP. In these regards, SSP electrophoretic mobility models presented by Ohshima [20–25] for the low charge regime are useful, where the particle core is present and the flow of the BGE solution in the polyampholyte layer is allowed. In [37], we study the electrophoretic mobility of BSA through the SSP model for different pH values to visualize this protein denaturation in the presence of a particle core. In this regard, it must be observed that experimentally measured mobilities of proteins are necessary for the determination of their electrokinetic and hydrodynamic parameters. Therefore, in the framework of the experimental CZE technique, it is required to put emphasis in that the mobilities have to be reported at well-defined values of pH, ionic strength, and temperature of BGEs.

4 Concluding remarks

The electrophoretic mobility expression of the SPP in the low charged regime is shown to be useful to physically interpret both denatured and near-native collapsed states of proteins. It is found that (i) the native and denatured states of globular BSA and STN proteins are modeled well as SPP within a wide range of pH, (ii) convective fluxes inside these proteins can be enhanced for the denatured states due to the increases of polypeptide porosity and permeability, where the friction fractal dimension also takes values above the Flory theta point, (iii) in the context of the present work the permeability, porosity, and packing fractal dimension of the polypeptide chain become relevant transport and structural properties of proteins when the SPP is used to model their electrophoretic mobility. Thus, the SPP model introduces a new "screening" parameter that is not present in the previous AHP model with occlude water. This implies that when flow occurs through the particle the permeability must be accounted as an additional transport property. In this regard, future research will be required to elucidate the full range of g_f relating to particle type (from collapsed to free draining chain). Thus, g_f is defining the Mark–Houwink exponent ν of the intrinsic viscosity that may vary from 0 to 2, but the physics underlying these results for charged chains still remains under study, mainly when this exponent takes values higher than 4/5, what is equivalent to $g_f > 3/5$. In general, each particle type allows explanations of different phenomena present in the complex protein system.

Further, electrophoretic mobility data of BSA and STN for different protocols demonstrate through the SPP model when the average regulating ⟨pH⟩ of protein domain is lower and higher than the bulk pH, having as pivot the p*I*. Finally, it is relevant to point out that the experimentally measured mobilities of proteins at well-defined pH, ionic strength, and temperature are necessary for the determination of their electrokinetic and hydrodynamic parameters.

Authors wish to thank the financial aid received from Universidad Nacional del Litoral, Santa Fe, Argentina (CAI+D 2009), and CONICET (PIP 112-200801-01106).

The authors have declared no conflict of interest.

© 2013 WILEY-VCH Verlag GmbH & Co. KGaA, Weinheim

5 References

[1] Dolník, V., *Electrophoresis* 2008, *29*, 143–156.

[2] El Rassi, Z., *Electrophoresis* 2010, *31*, 174–191.

[3] Selvaraju, S., El Rassi, Z., *Electrophoresis* 2012, *33*, 74–88.

[4] Kašička, V., *Electrophoresis* 2010, *31*, 122–146.

[5] Kašička, V., *Electrophoresis* 2012, *33*, 48–73.

[6] Deiber, J. A., Piaggio, M. V., Peirotti, M. B., *Electrophoresis* 2011, *32*, 2779–2787.

[7] Deiber, J. A., Peirotti, M. B., Piaggio, M. V., *Electrophoresis* 2012, *33*, 990–999.

[8] O´Brien, R. W., White, L. R., *J. Chem. Soc. Faraday Trans.* 1978, *74*, 1607–1626.

[9] Allison, S. A., *Macromolecules* 1996, *29*, 7391–7401.

[10] Allison, S. A., *Biophys. Chem.* 2001, *93*, 197–213.

[11] Henry, D. C., *Proc. R. Soc. Lond. Ser. A* 1931, *133*, 106–129.

[12] Piaggio, M. V., Peirotti, M. B., Deiber, J. A., *Electrophoresis* 2005, *26*, 3232–3246.

[13] Piaggio, M. V., Peirotti, M. B., Deiber, J. A., *Electrophoresis* 2007, *28*, 2223–2234.

[14] Peirotti, M. B., Piaggio, M. V., Deiber, J. A., *J. Sep. Sci.* 2008, *31*, 548–554.

[15] Piaggio, M. V., Peirotti, M. B., Deiber, J. A., *Electrophoresis* 2009, *30*, 2328–2336.

[16] Piaggio, M. V., Peirotti, M. B., Deiber, J. A., *J. Sep. Sci.* 2010, *33*, 2423–2429.

[17] Xin, Y., Mitchell, H., Cameron, H., Allison, S. A., *J. Phys. Chem. B* 2006, *110*, 1038–1045.

[18] Pei, H., Xin, Y., Allison, S. A., *J. Sep. Sci.* 2008, *31*, 555–564.

[19] Pei, H., Allison, S., *J. Chromatogr. A.* 2009, *1216*, 1908–1916.

[20] Ohshima, H., *J. Colloid Interf. Sci.* 1994, *163*, 474–483.

[21] Ohshima, H., *Adv. Colloid Interf. Sci.* 1995, *62*, 189–235.

[22] Ohshima, H., *J. Colloid Interf. Sci.* 2000, *228*, 190–193.

[23] Ohshima, H., *Electrophoresis* 2006, *27*, 526–533.

[24] Ohshima, H., *Colloid Polym. Sci.* 2007, *285*, 1411–1421.

[25] Ohshima, H., *Sci. Technol. Adv. Mater.* 2009, 063001.

[26] Duval, J. F. L., Ohshima, H., *Langmuir* 2006, *22*, 3533–3546.

[27] Chou, C.-H., Hsu, J.-P., Kuo, C.-C., Ohshima, H., Tseng, S., Wu, R. M., *Colloid Surface B* 2012, *93*, 154–160.

[28] Hill, R. J., Saville, D. A., Russel, W. B., *J. Colloid Interf. Sci.* 2003, *258*, 56–74.

[29] Allison, S., Wall, S., Rasmusson, M., *J. Colloid Interf. Sci.* 2003, *263*, 84–98.

[30] Hill, R. J., Saville, D. A., *Colloid Surface A* 2005, *267*, 31–49.

[31] Ohshima, H., *Colloids Surf. A: Physicochem. Eng. Aspects* 2011, *376*, 72–75.

[32] Veerapaneni, S., Wiesner, M. R., *J. Colloid Interf. Sci.* 1996, *177*, 45–57.

[33] Kuntz, I. D., *J. Am. Chem. Soc.* 1971, *93*, 514–516.

[34] Kuntz, I. D., *J. Am. Chem. Soc.* 1971, *93*, 516–518.

[35] Piaggio, M. V., Peirotti, M. B., Deiber, J. A., *Electrophoresis* 2007, *28*, 3658–3673.

[36] Fennema, O., in: Whitaker, J. R., Tannenbaum, S. R. (Eds.), *Food Proteins*, AVI Publishing, Connecticut 1977, pp. 50–90.

[37] Deiber, J. A., Piaggio, M. V., Peirotti, M. B., *Electrophoresis* 2013, *34*, 708–715.

[38] Menon, M. K., Zydney, A. L., *Anal. Chem.* 1998, *70*, 1581–1584.

[39] Kálmán, F., Ma, S., Fox, R. O., Horváth, C., *J. Chromatogr. A* 1995, *705*, 135–154.

[40] Hermans, J. J., Fujita, H., *Koninkl. Ned. Akad. Wetenschap. Proc. Ser. B* 1955, *58*, 182–187.

[41] Howells, I. D., *J. Fluid Mech.* 1974, *64*, 449–475.

[42] Hinch, E. J., *J. Fluid Mech.* 1977, *83*, 695–720.

[43] Kim, S., Russel, W. B., *J. Fluid Mech.* 1985, *154*, 269–286.

[44] Happel, J., *AICH J.* 1958, *4*, 197–201.

[45] Makino, K., Ohshima, H., *Sci. Technol. Adv. Mater.* 2011, 023001.

© 2013 WILEY-VCH Verlag GmbH & Co. KGaA, Weinheim